Catena 163 (2018) 361–377

Contents lists available at ScienceDirect

Catena

journal homepage: www.elsevier.com/locate/catena

Geomorphic evolution of the Yellow River Delta: Quantification of basin-scale natural and anthropogenic impacts

Chao Jiang[a,b], Shenliang Chen[a,*], Shunqi Pan[b], Yaoshen Fan[a], Hongyu Ji[a]

[a] State Key Laboratory of Estuarine and Coastal Research, East China Normal University, Shanghai 200062, China
[b] Hydro-environmental Research Centre, School of Engineering, Cardiff University, Cardiff CF24 3AA, UK

ARTICLE INFO

Keywords:
Yellow River
Delta
Geomorphic evolution
Natural impact
Anthropogenic impact

ABSTRACT

The intensified impacts of both natural and anthropogenic processes in river basins on the sustainabilities of river deltas worldwide have necessitated serious international socioeconomic and environmental concerns. The Yellow River Delta (YRD), which formed within a relatively weak coastal dynamic environment, provides an excellent opportunity for a quantitative study of basin-scale natural and human influences on deltaic transformation. An examination of long-term bathymetric data demonstrates that the annual volumetric change of the YRD has experienced a statistically distinct declining trend during 1977–2005 with substantial inter-annual variations. Consequently, the decadal geomorphic evolution of the YRD has successively undergone three stages, namely, quick, stable and slow accumulation stages. Taking the fluvial supply as a link in combination with long-term hydro-meteorological data, the geomorphologic processes of the YRD are closely associated with the rainfall, air temperature and water diversion within the Yellow River catchment. A significant quantitative relationship exists between the deltaic land accretion and basin controls, indicating that annual morphological change will decrease by 4×10^8 m^3/yr with every decrease of 100 mm/yr in annual precipitation, decline by 2.49×10^8 m^3/yr with every increase of 1 °C/yr in annual air temperature, and diminish by 1×10^8 m^3/yr with every increase of 100×10^8 m^3/yr in annual water abstraction. Further non-dimensional analysis reveals that 50.55%, 36.26% and 13.19% of the inter-annual variation of the morphological change can be attributed to inter-annual variations of the precipitation, air temperature and water diversion, respectively. Natural environmental changes can account for 86.81% of the overall variations, while human-induced changes can explain the rest. Moreover, the contributions from rainfall, air temperature and water diversion to the decadal landform evolution transition from quick accumulation to stable accumulation were estimated as 46.59%, 35.23% and 18.18%, respectively, and their respective contributions to the transition to the subsequent slow accumulation stage were 2.09%, 92.67% and 5.24%. The natural contributions to the inter-decadal shifts were calculated as 81.82% and 94.76%, which are much greater than the respective human-related contributions of 18.18% and 5.24%. Our quantification results highlight that since the late 1970s, the changes of natural environment throughout the watershed have played a strikingly important role in both the inter-annual and inter-decadal changes of the sedimentary processes of the YRD. This study provides valuable quantitative references for the validation of basin-delta process-based research and for the sustainable development of the YRD. Furthermore, the YRD can be regarded as a typical case for deltaic systems that are currently being subjected to catchment-scale natural and anthropogenic influences, thereby suggesting the direction of future research.

1. Introduction

River deltas formed as a result of the accumulation of substantial quantities of terrestrial sediments near estuaries are of great importance from a human perspective because they are host to numerous major cities, encompass vibrant wetland ecosystems and provide abundant sediment-associated resources for the global biogeochemical cycle (Overeem and Brakenridge, 2009; Syvitski, 2008; Wright, 1977). Understanding the transformations of river deltas affected by global environmental changes has been set as a goal of the International Geosphere Biosphere Programme, and consequently raised strong coordinated international efforts (Holligan and Boois, 1993; Syvitski et al., 2009). Generally, the accretion of land within river deltas crucially depends on the fluvial material supply, namely, water and sediment discharges into the sea (Saito et al., 2001), and the coastal environment of the receiving sea, including the tidal regime and wave

* Corresponding author.
E-mail address: slchen@sklec.ecnu.edu.cn (S. Chen).

https://doi.org/10.1016/j.catena.2017.12.041
Received 18 July 2017; Received in revised form 27 December 2017; Accepted 31 December 2017
Available online 05 January 2018
0341-8162/

climate (Galal and Takewaka, 2011). Other than coastal dynamics, river hydrological conditions vary radically and rapidly at inter-annual and longer timescales due to natural (e.g., rainfall and air temperature) and human-induced (e.g., dam and reservoir operations and implementations of water-soil conservation measures) environmental changes in river basins (Liu et al., 2014b; Syvitski and Milliman, 2007; Tian et al., 2016; Walling and Fang, 2003). Here, a river basin is defined as a river catchment area where water collects and drains off. In recent decades, the quantity of terrestrial materials transported into the oceans through many large rivers, including the Mississippi River, the Mekong River, the Pearl River, the Yangtze River and the Yellow River (Meade and Moody, 2010; Wang et al., 2011), has drastically declined, thereby exacerbating the vulnerabilities of estuarine sedimentary systems (Giosan et al., 2014; Tessler et al., 2015). Under the combined influences of natural processes and human activities throughout watersheds, most deltas face threats represented by the erosional retreat of shorelines, the recession of wetland ecosystems and the destruction of coastal infrastructures (Syvitski, 2008; Syvitski et al., 2009).

The temporal variations of basin natural and human-related factors and their spatial variations play extremely important and complex roles in runoff generation and sediment yield within a catchment and indirectly affect the deltaic geomorphological processes (Syvitski and Milliman, 2007; Wang et al., 2007; Walling and Fang, 2003). Therefore, the identification of basin controls on the deltaic evolution and the clarification of their relative quantitative impacts are both of great challenge, which have been inadequately addressed to date. In addition, a comprehensive quantification of the relationship between deltaic and basin processes is urgently needed to maintain or restore the sustainabilities of river deltas. Process-based numerical models, which are being increasingly utilized to simulate the short-term morphodynamic evolution of river deltas, appear to be both inefficient and inaccurate at the long-term scale for several reasons, including fugitive meteorological conditions, irregular basin-scale human interventions, strong couplings between river hydrological processes and channel bed evolutionary processes, complex river-ocean interactions and massive data processing requirements (Fagherazzi et al., 2015; Lespinas et al., 2014; Santos et al., 2014; Wang et al., 2006a). In contrast, multivariate statistical analysis could represent a practical approach for determining the dominant basin-related drivers of deltaic transformations, and differentiating their respective impacts on the deltaic evolution at multiple timescales by relating morphological changes to macro-scale influences from a statistical perspective. Among the worldwide-renowned deltas, the Yellow River Delta (YRD) in China provides an ideal site for such a statistically quantitative study, which could be a reference for similar deltaic systems.

Once hailed as the world's most rapidly constructive delta (Xu et al., 2002), the YRD formed from a large and heavily sediment-laden river, namely, the Yellow River, within a micro-tidal estuary characterized by weak wave activity (Hu et al., 1996; Ren and Shi, 1986). Over the past few decades, the hydrological processes of the Yellow River have been subjected to enormous influences from natural and human-induced environmental changes within the Yellow River catchment (Jiang et al., 2017; Wang et al., 2006b, 2007; Xu, 2005), thereby triggering profound morphological and ecological responses of the YRD (Cui et al., 2013; Peng et al., 2010). The water and sediment discharges of the Yellow River system have been intensively monitored since the 1950s. Similarly, the basin-scale precipitation, earth surface air temperature and various types of human activities have been observed since the 1960s. A series of high-resolution satellite images and detailed underwater bathymetric soundings have been acquired throughout the YRD since the 1970s. Collectively, these unique and valuable long-term datasets make it possible to reliably and statistically isolate the basin-scale natural and human-related impacts on the land accretion of the YRD in greater detail than most other river deltas. Previous extensive qualitative descriptions have been provided for the interrelations between the evolution of the YRD and natural and anthropogenic changes within the catchment (Kong et al., 2015; Peng and Chen, 2010; Yu et al., 2011; Zhou et al., 2015), but quantitative analyses have received much less attention. Xu (2006, 2008) quantitatively linked the coastline migration of the YRD to basin influences and performed estimates of both natural and human contributions to the inter-annual variations of deltaic morphological changes. However, these investigations were insufficient, as they considered only the transformation of the Yellow River Subaerial Delta (YRAD) while ignoring that of the Yellow River Submerged Delta (YRSD). However, the subaqueous delta is an indispensable component of a deltaic system, as it not only supports the subaerial delta but also reflects the principal outcome of river-ocean interactions (Elliott, 1989). Jiang et al. (2017) revealed a close association between the progradation of both the YRAD and the YRSD at an inter-annual timescale. Such a quantification is credible only when the topographic changes of the YRAD and the YRSD are investigated in tandem. In addition, the impacts of catchment-scale natural processes and human activities on the transition of medium-term geomorphic evolution of the YRD also require some understanding. Jiang et al. (2017) and Wang et al. (2007) evaluated the contributions of various basin factors to the change in fluvial sediment supply of the Yellow River over different decades and indirectly and qualitatively demonstrated the association between basin influences and the medium-term evolution of the YRD, but their proposed direct quantitative relationships still needs to be further studied.

Hence, the main objectives of our research are to: 1) examine the volumetric change of the YRD (1977–2005), including the YRAD and YRSD, 2) identify the natural and human drivers within the catchment that dominate the deltaic transformation using fluvial input as a link, 3) establish a quantitative association between the deltaic morphological changes and influential basin parameters, and 4) quantify the natural and anthropogenic contributions to the inter-annual and inter-decadal changes of the deltaic geomorphological processes. This research could be conducive to bridge the knowledge gap between short-term seasonal and long-term (i.e., centennial- to millennial-scale) sedimentary evolutionary trends of the YRD under changes to the catchment environment. Moreover, the insights gained from this study could provide policy makers with valuable quantitative references for the sustainability of the YRD and guide public concerns regarding the further development of other deltas.

2. Overview of the study area

As the second largest river in China, the Yellow River originates from the Qinghai-Tibet Plateau, loops around the Loess Plateau (LP), and then flows generally eastwards across alluvial plains into the Bohai Sea (Fig. 1a). The Yellow River is the largest contributor in Asia of fluvial sediments into the sea, and it ranks second globally in terms of the quantity of sediment discharged into the sea over the past millennium (Milliman and Meade, 1983). The Yellow River can be divided into three sections according to its geographic characteristics: the upper reaches, the middle reaches and the lower reaches (Fig. 1a). The average annual precipitation is highly variable across the river basin and ranges from 368 mm in the upper reaches to 530 mm in the middle reaches and to 670 mm in the lower reaches. The average annual air temperature varies from 1 °C to 4 °C in the upper reaches, from 8 °C to 14 °C in the middle reaches, and from 12 °C to 14 °C in the lower reaches (Chen et al., 2005). Over the past few decades, the average annual precipitation within the catchment has declined significantly while the average annual air temperature has increased markedly (Wang et al., 2013; Yao and Wu, 2014). During the latter half of the 20th century, a series of water-soil conservation measures were implemented within the middle reaches to improve the soil anti-erosion ability and prevent soil loss within the LP (Wang et al., 2007). By 2005, these erosion control practices, which included the construction of terraces, the implementation of reforestation and the planting of grass, had controlled an area of approximately 78,000 km^2 throughout the

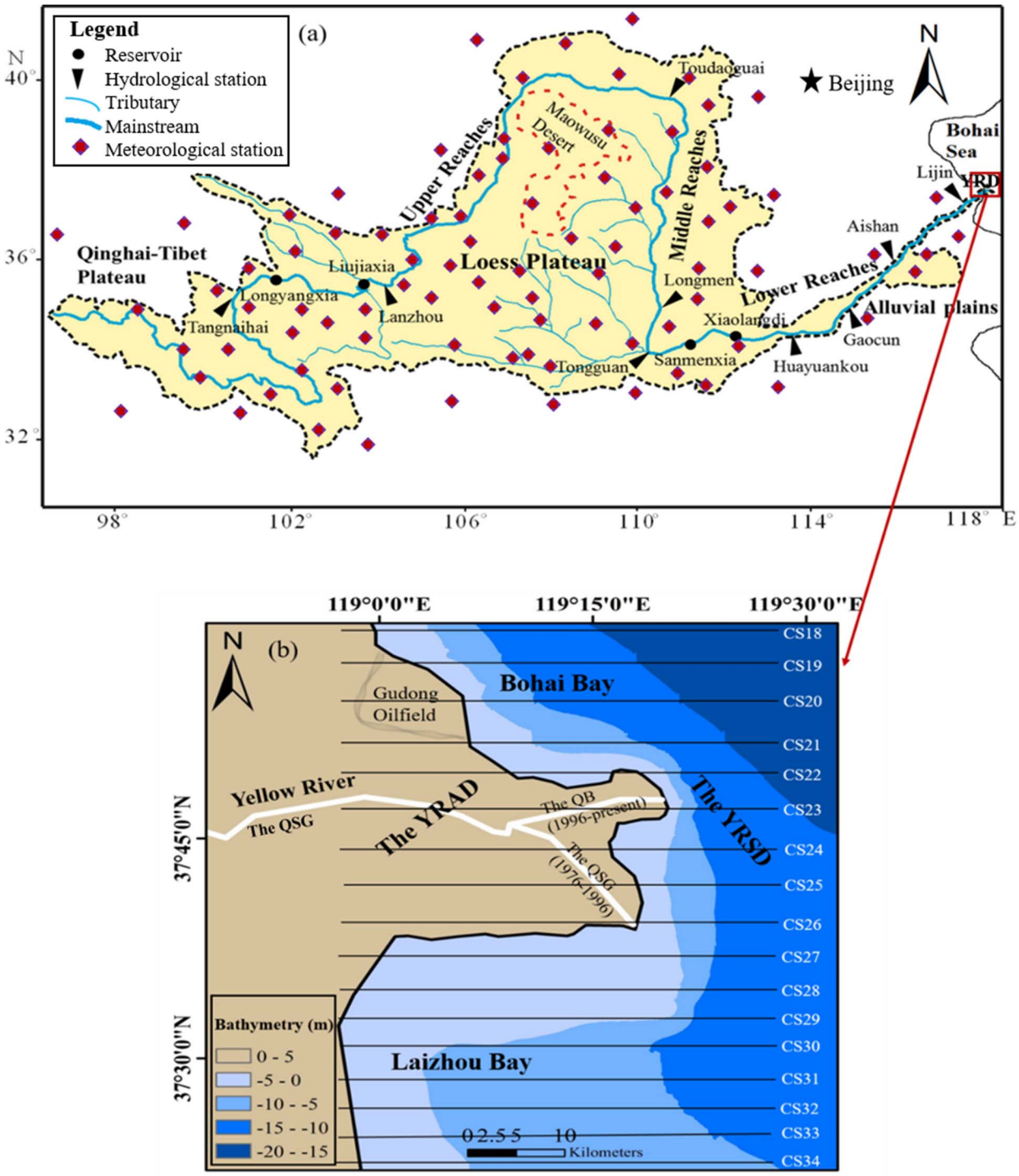

Fig. 1. a) Map of the Yellow River basin, with locations of major reservoirs, hydrological stations, tributaries and meteorological stations, as well as the YRD; b) Topographic map of the YRD (2005) with bathymetry measurement transections.

watershed (Yu et al., 2011). Meanwhile, water diversion efforts have been considerably intensified due to increasing water demands for living, irrigation, industrial production and dam operations (Peng et al., 2010). > 3380 reservoirs had been completed by 2004 within the drainage basin for a total storage capacity of about 563×10^8 m^3 (Yu et al., 2011). Among them, the Sanmenxia, Liujiaxia, Longyangxia and Xiaolangdi Reservoirs constitute the four major mainstream reservoirs (Fig. 1a) that came into operation in 1960, 1968, 1986 and 2000, respectively. The river discharge at the most downstream hydrological station, namely, the Lijin Hydrological Station (LJHS), has experienced a stepwise reduction since the 1950s, which is fundamentally attributable to natural and human-induced environmental changes (Liu et al., 2014a; Peng et al., 2010; Xu, 2003, 2005).

The YRD has been gradually formed in the western Bohai Sea (Fig. 1a) ever since the Yellow River migrated its main watercourse from the Yellow Sea to the Bohai Sea in 1855 (Pang and Si, 1979). The YRD has since developed several deltaic lobes in the Bohai Sea due to the subsequent frequent shifts of its course (Pang and Si, 1979; Qiao et al., 2011). The progradation of the active delta lobe started in May 1976 coincident with the large-scale artificial movement of the outlet

from the Diaokou Channel to the Qingshuigou Channel (QSG). During the period of 1855–2000, the YRD has extended seawards over a vast fan-shaped zone, thereby occupying a land area of 5129 km^2 and a stretch of coastline 227 km long (Chu et al., 2006). Since oil and natural gas resources were discovered beneath the YRD in the 1960s, astonishing economic progress has been registered in the region (Xu et al., 2002). In addition, the wetlands developed within the YRD constitute a vital habitat for many rare and endangered migrating bird species, including the red-crowned crane, hooded crane, Siberian crane, oriental stork, black stork and golden eagle (Zhang et al., 1998). The marsh and swamp plant communities in the wetlands that were established initially upon a substrate of clastic sediments derived from the Yellow River maintain a high level of productivity (Cui et al., 2013). Due to the great socioeconomic and ecological importance of the YRD, environmental changes of the delta influenced by the natural and human-induced reductions of fluvial supply have aroused serious concerns from various disciplines (Pang et al., 2013; Peng et al., 2013; Sun et al., 2015). It should be noted that the YRD investigated in this paper is otherwise referred to as the active delta lobe in Fig. 1b, which is adjacent to the Bohai Bay and Laizhou Bay. The beak-shaped river mouth shown in Fig. 1b was formed as a result of a minor artificial movement of the QSG outlet to the 8th section of the QSG (QB) in 1996 to facilitate the operation of the Kendong Oilfield. Generally, the YRD consists of the YRAD and the YRSD. Here, the YRAD is defined as the terrestrial component above the 0 m isobath, while the YRSD is deemed to be the area where the bathymetric level is between the isobaths of 0 m and approximately −15 m. The majority of fluvial sediments have been accumulated close to the river mouth, resulting in the construction of a steep subaqueous slope above the −10 m isobath (Peng et al., 2013; Wu et al., 2017). The YRD is a newly born and highly constructive sedimentary system with uncompacted sedimentary deposits that tend to be easily eroded and are subject to subsidence (Chu et al., 2006). The dry bulk density of the underwater sediment was estimated at approximately 1.10–1.50 × 10^3 kg/m^3 (He et al., 2017; Sun et al., 1993). The region is characterized by the control of a warm-temperate semi-humid continental monsoon climate with distinct seasonal variations (Sun et al., 2014). The coastal dynamic environment around the YRD operates under a relatively weak tidal regime and wave climate (Chu et al., 2006; Hu et al., 1996). The tidal currents off the estuary flow southwards during the flood tide and northwards during the ebb tide with an average velocity of 0.5–1.0 m/s (Cheng and Cheng, 2000). The wind-driven residual current usually moves northwards during the winter and southwards during the summer with a mean velocity of 0.1–0.25 m/s (Pang and Si, 1979).

3. Data and methods

Bathymetric data obtained from the Yellow River Conservancy Commission were surveyed along 17 cross-shore subaqueous profiles numbered from CS18 to CS34 (Fig. 1b) in each October during the periods of 1976–1982, 1985–1987, 1989–1991, 1993–1999, and 2001–2005. Topographic data were collected at an interval of approximately 500 m along each transect starting from a water depth of ~2 m and extending seawards to a water depth of ~15 m using an SDH-13D digital echo sounder and a UHF-547 microwave apparatus. Due to the lack of water depths shallower than ~2 m, multi-temporal remote-sensing data of Landsat Multispectral Scanner (MSS), Landsat Thematic Mapper (TM) and Landsat Enhanced Thematic Mapper Plus (ETM +) satellite images archived by the Earth Resources Observation and Science (EROS) Center (http://glovis.usgs.gov/) were utilized to obtain the shoal topography. The detailed information of the satellite images are shown in Table 1. Since the remnant surface water of a mudflat can remain for long periods during a tidal cycle, the high-water line is considered the wet/dry line between a tidal flat and land (Li and Gong, 2016; Ryu et al., 2002). Using a supervised clarification method, the wet/dry line can be easily extracted with a relatively high accuracy from satellite images taken at low tide (Fan et al., 2009; Li and Gong, 2016). Since the effects of wave runoff can be ignored along the muddy coastline of the YRD characterized by weak wave conditions, the wet/dry line can be critically determined using the high-tide height. According to local tidal data, the high-tide heights during the acquisition dates of the satellite images listed in Table 1 were close to the 0 m isobath. Thus, the wet/dry lines extracted from the satellite images can be adopted to approximately represent the 0 m isobaths. In addition, the likely errors involved are mainly associated with the differences between the locations of the high-tide line (i.e., the wet/dry line) and the 0 m isobath and with the extraction process of the wet/dry line. With regard to the latter, all of the images were geo-referenced and rectified following the procedure suggested by Serra et al. (2003). To generate topographic maps of the YRD for different years, the measured and extracted bathymetric data referenced to the Yellow Sea Datum were interpolated into a grid with 50 m by 50 m cells using the Kriging interpolation in the DTM (digital terrain model) within ArcGIS 10.1. The maps of bathymetric changes of the YRD between adjacent observation years were then digitized by deducing the later depth from the earlier depth, which delineate the vertical accretion/erosion thickness and the horizontal accretion/erosion areas between different periods. The volumetric changes of the YRD, which includes the YRAD and YRSD, were further calculated according to the total volume of accretion minus that of erosion. Note that the volumetric changes were interpolated over yearly intervals by considering the year water discharges as weights when the time interval between two adjacent topographic maps is longer than 1 year, according to the close relationship between coastline change and river flow discharge (Cui and Li, 2011; Xu, 2002).

Additionally, annual water and sediment discharges during 1977–2005 measured at the LJHS by the Yellow River Conservancy Commission are obtained from the River Sediment Bulletin of China. Annual precipitation and air temperature data during 1977–2005 that were observed at > 80 meteorological stations distributed broadly within the catchment (Fig. 1a) were provided by the China Meteorological Administration (http://www.cma.gov.cn/english/). Since the magnitudes of the precipitation and air temperature in the lower reaches are higher than those in the upper and middle reaches, and since the controlling area of the lower reaches is much smaller than those of the upper and middle reaches, an arithmetic average of the meteorological station data cannot accurately account for the spatial averages of meteorological elements. Thus, basin-scale annual precipitation and air temperature averages were determined via the Kriging interpolation of annual precipitations and air temperatures from the meteorological stations in ArcGIS 10.1. The annual net water diversions and average annual water reductions induced by water-soil conservation measures throughout the watershed (1970–2005) were primarily obtained from the literatures (Hu et al., 2008; Tang, 2004; Xu, 2008). Here, the net water abstraction refers to the quantity of water diverted from the river for domestic, agricultural and industrial consumption and dam operations minus the quantity of water returned to the river after use. Further statistical analyses of the hydro-meteorological and bathymetric time-series data were mainly conducted using the nonparametric Mann-Kendall (MK) test and the SPSS 18.0 software.

4. Results

4.1. Geomorphic evolution of the YRD

Previously, Jiang et al. (2017) analysed the medium-term (decadal) geomorphic evolutionary characteristics of the YRSD and quantified the annual volumetric changes of the YRSD. However, their study did not provide an understanding of the short-term (inter-annual) morphological change features of the YRD and evaluate annual volumetric changes of the YRD (V). Fig. 2 shows the spatial distributions of deposition and erosion throughout the YRD and the movements of 0 m

Table 1
The detailed information of satellite images in the present study.

Acquisition date	Image type	Resolution (m)	Acquisition date	Image type	Resolution (m)
02/06/1976	MSS	60	08/06/1993	TM	30
10/05/1977	MSS	60	30/08/1994	TM	30
14/05/1978	MSS	60	18/09/1995	TM	30
11/07/1979	MSS	60	02/07/1996	TM	30
14/07/1980	MSS	60	07/09/1997	TM	30
12/06/1981	MSS	60	25/08/1998	TM	30
08/10/1982	MSS	60	07/10/1999	TM	30
06/09/1985	TM	30	06/06/2001	ETM +	30
05/06/1986	TM	30	28/08/2002	ETM +	30
07/05/1987	TM	30	27/05/2003	TM	30
15/07/1989	TM	30	04/10/2004	TM	30
16/06/1990	TM	30	03/07/2005	ETM +	30
05/07/1991	TM	30			

isobath between different short periods during 1976–2005. Fig. 2 clearly demonstrates that the geomorphic evolutionary processes of the YRD over the study period were extremely complicated and were characterized by irregular distributions and shifts of deposition and erosion. In general, a distinct deposition zone appeared around the river mouth with the highest vertical accretion rate of approximately 1.20 m/yr; this zone migrated northwards in 1976–1982, followed by southward movement in 1982–1995 and finally a northward shift in 1995–2005. Shifts in the deposition/erosion patterns throughout the YRD were coincident with the movement of the watercourse, particularly around the previous river mouth. For instance, since the river was diverted to the QB in 1996, the former QSG estuary has transitioned from progradation to recession due to the interruption of its fluvial supply. From 1976 to 1996, the 0 m isobath of the YRD extended approximately 30 km towards the southeast at a rate of ~1.58 km/yr around the QSG outlet into the Bohai Sea. After 1996, the 0 m isobath started to extend towards the northeast around the QB outlet and to retreat around the previous QSG outlet. During the period of 1996–2005, the 0 m isobath extended ~8.93 km seaward around the QB outlet at a rate of 0.89 km/yr, which is 43.67% lower than the rate in 1977–1995.

The time series of V for the period of 1977–2005 shown in Fig. 3 were obtained based on the topographic changes throughout the YRD shown in Fig. 2. Long-term change in V presented a tendency to descend at an average rate of 0.19×10^8 m^3/yr. The value of V ranged from -3.70×10^8 m^3/yr in 1980 to 10×10^8 m^3/yr in 1983 with substantial inter-annual variations. A recession of the YRD (negative values of V) occurred in 1980, 1986, 1987, 1997, 2000, 2001, 2002 and 2003. To examine the geomorphic evolution of the YRD at the medium-term scale, the period of 1977–2005 was divided into three successive time ranges at approximate decadal intervals, namely, 1977–1985, 1986–1995 and 1996–2005. The averages of V among the three different decades are reflected by solid red lines in Fig. 3, which indicate a remarkable decrease. Specifically, the average value of V was 5.72×10^8 m^3/yr in 1977–1985; it declined by 33.55% to 3.80×10^8 m^3/yr in 1986–1995 before finally reaching 0.99×10^8 m^3/yr in 1996–2005 with a further reduction of 73.87%. According to the average values of V, the decadal landform evolution of the YRD has successively experienced three stages during 1977–2005, namely, rapid accumulation in 1977–1985, stable accumulation in 1986–1995 and slow accumulation in 1996–2005.

4.2. Deltaic morphological response to river hydrological changes

A river constitutes the major pathway for the delivery of fresh water and terrestrial materials. Fig. 4a shows the temporal variations of the annual water discharge (Q) and the sediment load (Q_s) at the LJHS between 1977 and 2005. Given that the LJHS is situated near the estuary, Q and Q_s can be approximately regarded as the water and sediment discharges into the Bohai Sea, respectively. The long-term changes in Q and Q_s both exhibit stepwise declining trends with respective mean reduction rates of 8.47×10^8 m^3/yr and 0.28×10^8 t/yr. Substantial inter-annual variations exist in both Q and Q_s, which were roughly synchronous. In the years of 1981, 1983, 1994, 1998 and 2003, the peaks of Q_s appeared simultaneously with the peaks of Q. The values of Q_s in drought years (e.g., 1980, 1987, 1991 and 1997) were significantly lower than those in other years. The variation coefficient (C_v) can be utilized to evaluate the inter-annual variations of Q and Q_s, and C_v can be calculated using the following equation (Si et al., 1999):

$$C_v = \sqrt{\frac{\sum_{i=1}^{N}\left(\frac{x_i}{\overline{x}} - 1\right)^2}{N-1}} \quad (1)$$

where x_i, $\overline{x}$ and N represent the annual water discharge (annual sediment load), multi-year average water discharge (sediment load) and the length of the time series, respectively. The value of C_v ranges from 0 to 1, where larger values indicate greater inter-annual variations. The C_v values of Q and Q_s were calculated to be 0.68 and 0.73, respectively, indicating that the inter-annual variations of both Q and Q_s were considerable. The water and sediment discharges have been both intensively affected by natural and human-induced environmental changes within the catchment during the period of 1977–2005. A simple linear regression analysis was further applied to Q and Q_s, thereby revealing a close positive linear relationship between them (Fig. 4b). The regression equation can be expressed as

$$Q_s = 0.02Q + 0.10 \quad (2)$$

The correlation coefficient is 0.87, which is significant at a level of $p < 0.01$. Eq. (2) indicates that the annual sediment load into the sea ascends with an increase of the annual flow discharge. The strong correlation between Q and Q_s suggests that the water-sediment relationship at the end of the lower reaches was roughly stable in 1977–2005 and did not markedly change following the installation or implementation of hydraulic structures (e.g., the Longyangxia Reservoir and water-soil control practices) in the middle and upper reaches.

From a morphodynamic perspective, different hydrodynamic processes will dominate the dispersal of estuarine sediments with the consequent morphological development depending on the relative strength of the fluvial dynamics with respect to the coastal dynamics. In a relatively weak coastal dynamic environment, the response of land accretion of the YRD to significant hydrological changes in the river needs to be understood. Given the foregoing water-sediment relationship, the river flow discharge can be taken as the representative of the river hydrological environment. Based on the time series data of V and Q from 1977 to 2005, the temporal variations of deltaic transformation and river water supply were examined. As shown in Figs. 3 and 4a, the long-term changes in V and Q both indicate a descending tendency with

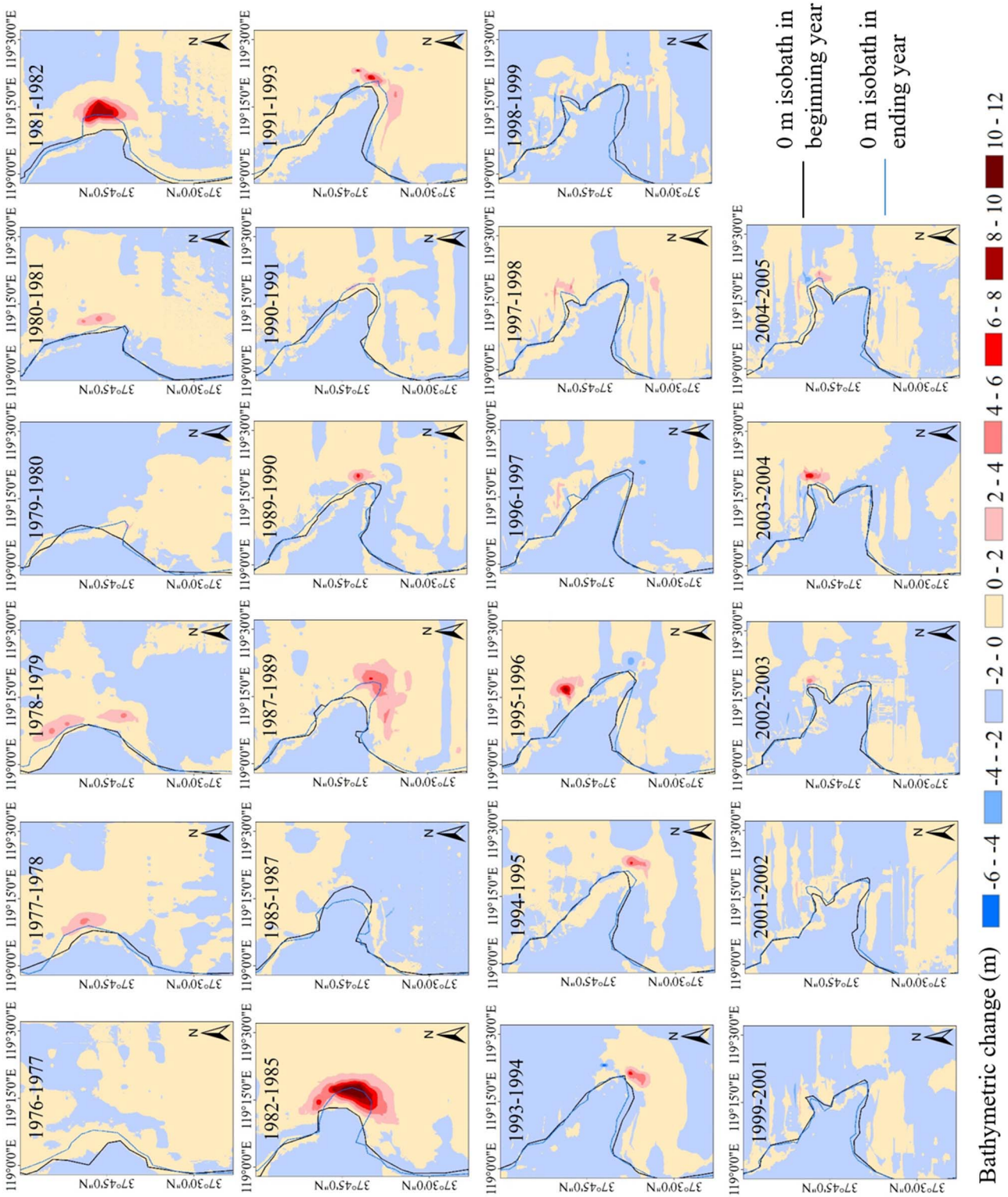

Fig. 2. Spatial variations of deposition-erosion pattern of the YRD between adjacent observation years.

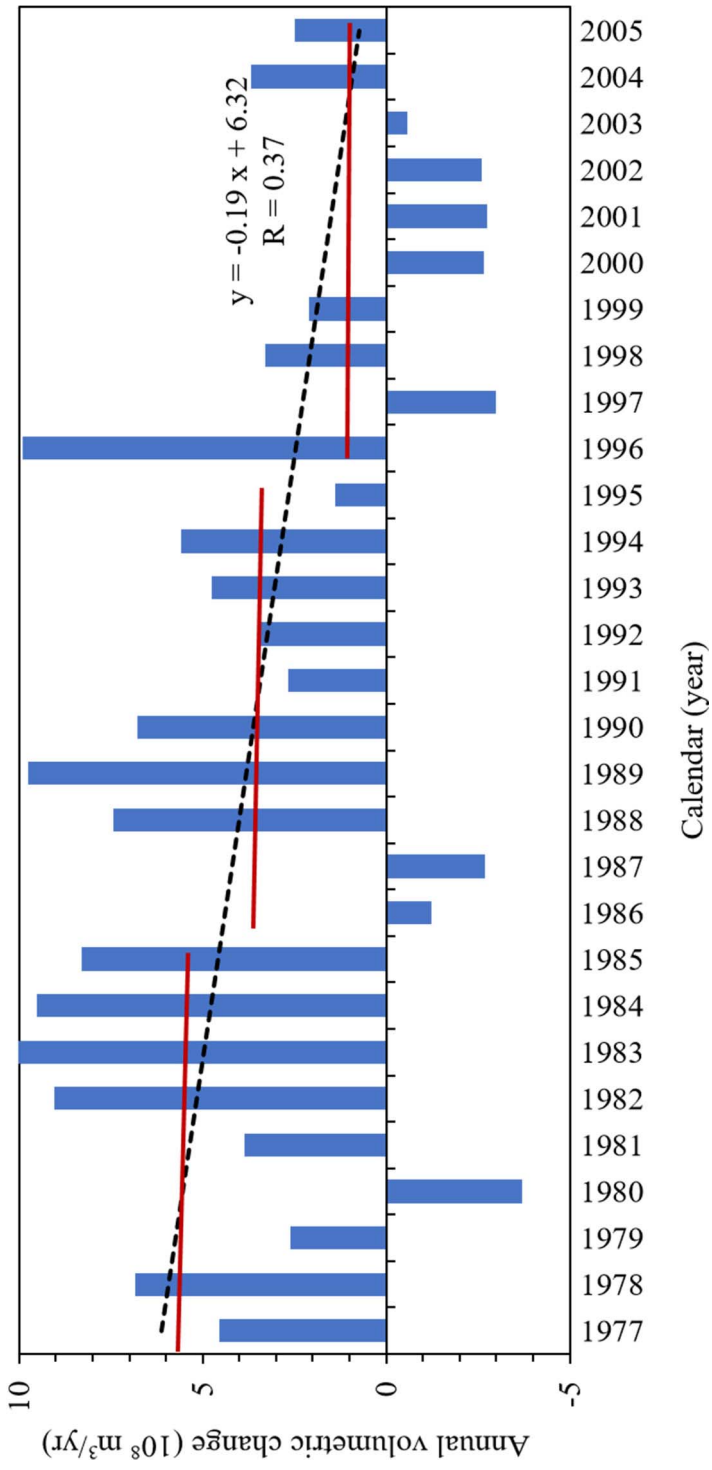

Fig. 3. Temporal variation of annual volumetric change of the YRD from 1977 to 2005 (the red constant line means average annual volumetric change for three decadal periods). (For interpretation of the references to color in this figure legend, the reader is referred to the web version of this article.)

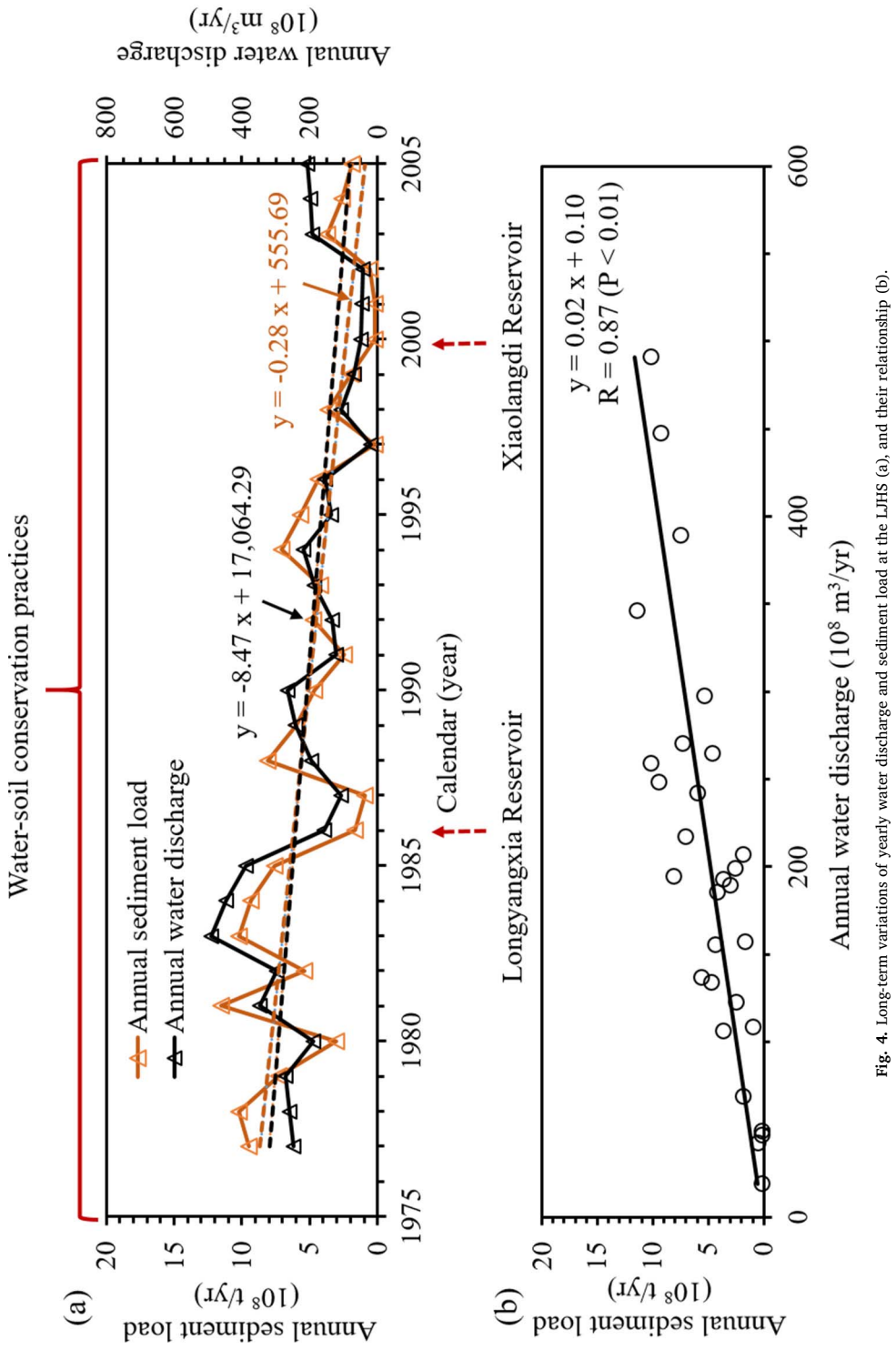

Fig. 4. Long-term variations of yearly water discharge and sediment load at the LJHS (a), and their relationship (b).

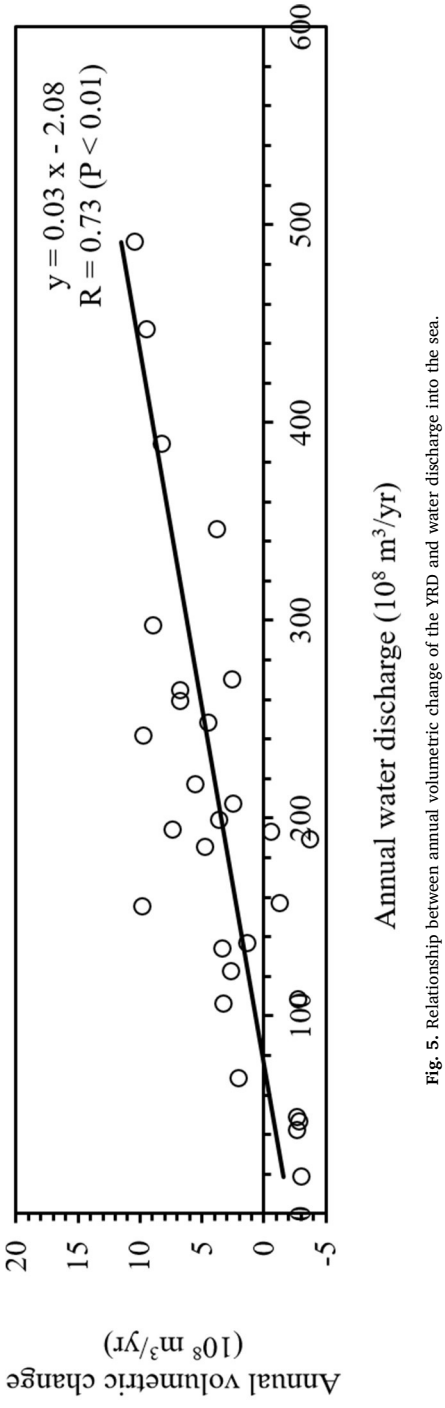

Fig. 5. Relationship between annual volumetric change of the YRD and water discharge into the sea.

substantial and roughly synchronous inter-annual variations. The relatively higher values of V correspond to relatively greater values of Q in the years of 1983, 1989, 1994, 1998 and 2004, and the relatively lower V values coincide with relatively smaller Q values in the years of 1980, 1987, 1991, 1997 and 2002. To further diagnose their association, the V data were regressed against those of Q using a simple linear regression (Fig. 5), revealing a close positive linear relationship between V and Q with a correlation coefficient of 0.73, which is significant at a level of $p < 0.01$. The linear regression equation can be expressed as

$$V = 0.03Q - 2.08 \quad (3)$$

The high correlation between V and Q reflects that the geomorphic evolution of the YRD critically depends on the water flux of the Yellow River into the sea at the annual timescale. The coefficient in Eq. (3) indicates that V will ascend by 3×10^8 m^3/yr with an increment in Q of 100×10^8 m^3/yr. The mechanism for the above relationship can be explained as follows. One the one hand, larger runoff rates will transport more terrestrial sediment into the deltaic sedimentary system, resulting in higher deposition. On the other hand, stronger fluvial dynamics will affect the coastal dynamics to some extent, altering the erosion caused by coastal processes. When the effect of the river supply just offsets that of the coastal dynamics, the YRD will be subjected to an accumulation/erosion equilibrium state. According to Eq. (3), the threshold of the river flow discharge for maintaining the sediment budget (V = 0) at the annual timescale is quantified as 69.33×10^8 m^3/yr. Cui and Li (2011) and Xu (2002) revealed a close association between the coastline migration of the YRD and the river water supply among different time ranges and estimated the critical amount of the water flux required for a balance between the extension and retreat of the shoreline as 76.70×10^8 m^3/yr during 1955–1989 and 85×10^8 m^3/yr during 1996–2005. The good consistency between the present and previous results can effectively support the reliability of our analysis.

4.3. Natural and human factors dominating deltaic transformation

The landform evolution of the YRD critically depends on the river discharge, which is highly affected by both natural and anthropogenic processes within the Yellow River catchment. Therefore, before the dominant natural and human drivers on the deltaic transformation can be identified, the primary factors that control the river flow discharge must be clarified.

The rainfall and earth surface air temperature are the two most frequently used natural indicators for the spatial and temporal variabilities in the global hydrological cycle, while water diversion projects and water-soil conservation measures constitute the two most influential human factors. Jiang et al. (2017) assumed that the rainfall, air temperature and water diversion are the primary controls on the water discharge. However, the interrelationships among these three variables have not been well analysed, and the effect of water-soil conservation practices on the water discharge has been ignored. To reveal the individual effects of the rainfall, air temperature, water diversion projects and water-soil conservation efforts on the river water supply, time series datasets of the annual water discharge and of the basin-scale annual precipitation, air temperature, water abstraction and water loss from water-soil conservation were examined. As indicated in Table 2, the multi-year average water reductions by water-soil conservation were significantly smaller than the multi-year average water discharges and water diversions, and the differences in the water reduction between adjacent periods were much below those of the water discharge and water diversion as well. In stark contrast to the water diversion, the water-soil conservation has contributed a negligible amount to the drastic reduction in the river flow discharge over the past few decades and thus cannot be considered a dominant human factor.

The time series of the basin-scale average annual precipitation (P),

Table 2
Average annual water discharges, water diversions and water losses from water-soil conservation in different periods.

Periods	Average annual water discharge (10^8 m^3/yr)	Average annual water diversion (10^8 m^3/yr)	Average annual water reduction by water-soil conservation (10^8 m^3/yr)
1970–1979	311.22	251.83	21.93
1980–1989	285.97	304.50	29.35
1990–1999	140.75	309.70	29.04
2000–2005	122.54	342.50	27.36

air temperature (T) and water diversion (Q_d) between 1977 and 2005 are shown in Fig. 6. It can be found from Figs. 4 and 6 that the temporal variation of P exhibited a downward trend with a mean annual reduction of 0.92 mm, while that of Q indicated a tendency to decrease at an average rate of 8.47×10^8 m^3/yr. Substantial inter-annual variations are observed in P and Q, which were roughly synchronous. For instance, a relatively high P occurred in 1983 with a value of 510 mm/yr corresponding to the highest Q of 491×10^8 m^3/yr. The lowest Q of 18.61×10^8 m^3/yr in 1997 coincided with a relatively low P of 360 mm/yr. Contrary to the declining trend of Q, the long-term change in T presented an apparent upward trend with a mean annual increase of 0.05 °C/yr. To some extent, the inter-annual variations of T also demonstrated a synchronicity with those of Q. For example, the relatively low Q of 106.20×10^8 m^3/yr corresponded with the highest T of 8.25 °C/yr in 1998. The peak of Q (491×10^8 m^3/yr) appeared in 1983 coincident with a relatively low T of 6.40 °C/yr. While the natural environment changed considerably during 1977–2005, human interventions (namely, water diversion projects) increased significantly. Compared with the mean reduction rate of Q, Q_d ascended at a smaller mean rate of 2.23×10^8 m^3/yr and reached its maximum value of 425×10^8 m^3/yr in 1989. Evidently, the river flow discharge has declined dramatically with a decrease of precipitation, an increase of air temperature and an increase of water diversion during 1977–2005. Table 3 shows the correlation coefficient matrix among all of these variables (P, T, Q_d and Q). Close relationships exist between Q and P, T and Q_d with respective correlation coefficients of 0.63, −0.67 and −0.58, all of which are significant at a level of $p < 0.01$.

To further determine the combined effect of these parameters on the river flow discharge, multiple regression analysis was conducted with the datasets in the period of 1977–2005. Given the low correlation coefficients among P, T and Q_d (Table 3), it is clear that no significant covariance exists among them. For this analysis, Q was taken as the dependent variable while P, T and Q_d were taken as the independent variables. The multiple regression equation can be established as follows:

$$Q = 655.95 + 1.06P - 92.59T - 0.88Q_d \quad (4)$$

The correlation coefficient is 0.88, which is significant at a level of $p < 0.01$. Eq. (4) indicates that Q increases with P and declines with both T and Q_d, and puts their association into a quantitative context. Using Eq. (4), we regressed the annual flow discharges from the annual precipitations, air temperatures and water diversions between 1977 and 2005, and then plotted the calculated values against the measured ones in Fig. 7. The predicted values are in close proximity to the observed ones, visually demonstrating that the rainfall, air temperature and water abstraction are the dominant factors that control the river water supply. Given the significant correlation between the water flux and the deltaic transformation, these three forcing factors can be considered the major natural and human controls on the evolution of the delta.

4.4. Quantitatively linking morphological change with influences

Multiple regression analysis was also conducted to quantify the respective impacts of various basin influences on the observed deltaic morphological changes. V was taken as the dependent variable, while P, T and Q_d were taken as the independent variables. The data in the period of 1977–2005 were available for this analysis for a total of 29 years. The multiple regression equation can be established as follows:

$$V = 5.88 + 0.04P - 2.49T - 0.01Q_d \quad (5)$$

The correlation coefficient is 0.77, which is significant at a level of $p < 0.01$. This high correlation suggests that the geomorphic evolution of the YRD at the annual timescale can be critically determined by the rainfall, air temperature and water abstraction throughout the drainage basin. Using Eq. (5), the future value of V can be estimated according to the predicted annual basin-scale P, T and Q_d.

In Eq. (5), it is evident that the coefficients of P, T and Q_d are considerably different, signifying that each of the contributions from the unit amounts of P, T and Q_d to V are distinctive. Eq. (5) indicates that the value of V ascends by 4×10^8 m^3/yr with every increase of 100 mm/yr in P, decreases by 2.49×10^8 m^3/yr with every increase of 1 °C/yr in T, and descends by 1×10^8 m^3/yr with every increase of 100×10^8 m^3/yr in Q_d. The above results provide quantitative references for the association between the variations in the deltaic evolution and the natural and anthropogenic changes within the catchment. These references will be conducive to the calibration of future basin-delta process-based research.

4.5. Natural and anthropogenic contributions to inter-annual and inter-decadal variations of morphological change

Corresponding to the inter-annual variations of precipitation, air temperature and water diversion (Fig. 6), the morphological change of the YRD has varied significantly at the inter-annual timescale during 1977–2005 (Fig. 3). The inter-annual changes of precipitation (ΔP), air temperature (ΔT), water diversion (ΔQ_d) and volumetric change (ΔV) between 1977 and 2005 were accordingly calculated and analysed. ΔV occurs as the combined result of ΔP, ΔT and ΔQ_d. To understand the natural and anthropogenic impacts on the inter-annual variations of the landform evolution during 1977–2005, we need to quantify the overall respective contributions from ΔP, ΔT and ΔQ_d to ΔV. Since the ranges of the absolute values of the independent variables in Eq. (5) differ from one another, the regression coefficients of these variables cannot directly reflect their relative contributions to the variation of the dependent variable. To address this issue, non-dimensional analysis was conducted in SPSS 18.0. The independent variables (namely, P, T, and Q_d) and dependent variables (namely, V) during the period of 1977–2005 were normalized to P′, T′, Q_d' and V′ using zero-mean normalization. The standardized multiple regression equation can be established as follows:

$$V' = 0.46P' - 0.33T' - 0.12Q_d' \quad (6)$$

where the coefficients of P′, T′ and Q_d' can generally reflect the respective absolute effects of ΔP, ΔT and ΔQ_d on ΔV. Assuming that the total contribution of ΔP, ΔT and ΔQ_d to ΔV is 100%, the relative contributions of the basin-scale rainfall, air temperature and water diversion to the inter-annual variation of the deltaic volumetric change can be estimated by considering the standardized regression coefficients in Eq. (6) to be weights. Consequently, the contributions from ΔP, ΔT and ΔQ_d accounted for 50.55%, 36.26% and 13.19%, respectively, of the inter-annual variation of ΔV within the period of 1977–2005. In terms of their impacts on the variation of the short-term (i.e., annual) landform evolution, the rainfall ranked first, followed by air temperature and then finally water diversion. Following further calculation, the total contribution from natural factors was 86.81% while that from human factors was 13.19%. Since the late 1970s, the inter-annual variation of natural environment in the Yellow River basin has played a more significant role in the inter-annual variation of geomorphological processes of the YRD than those of human intervention.

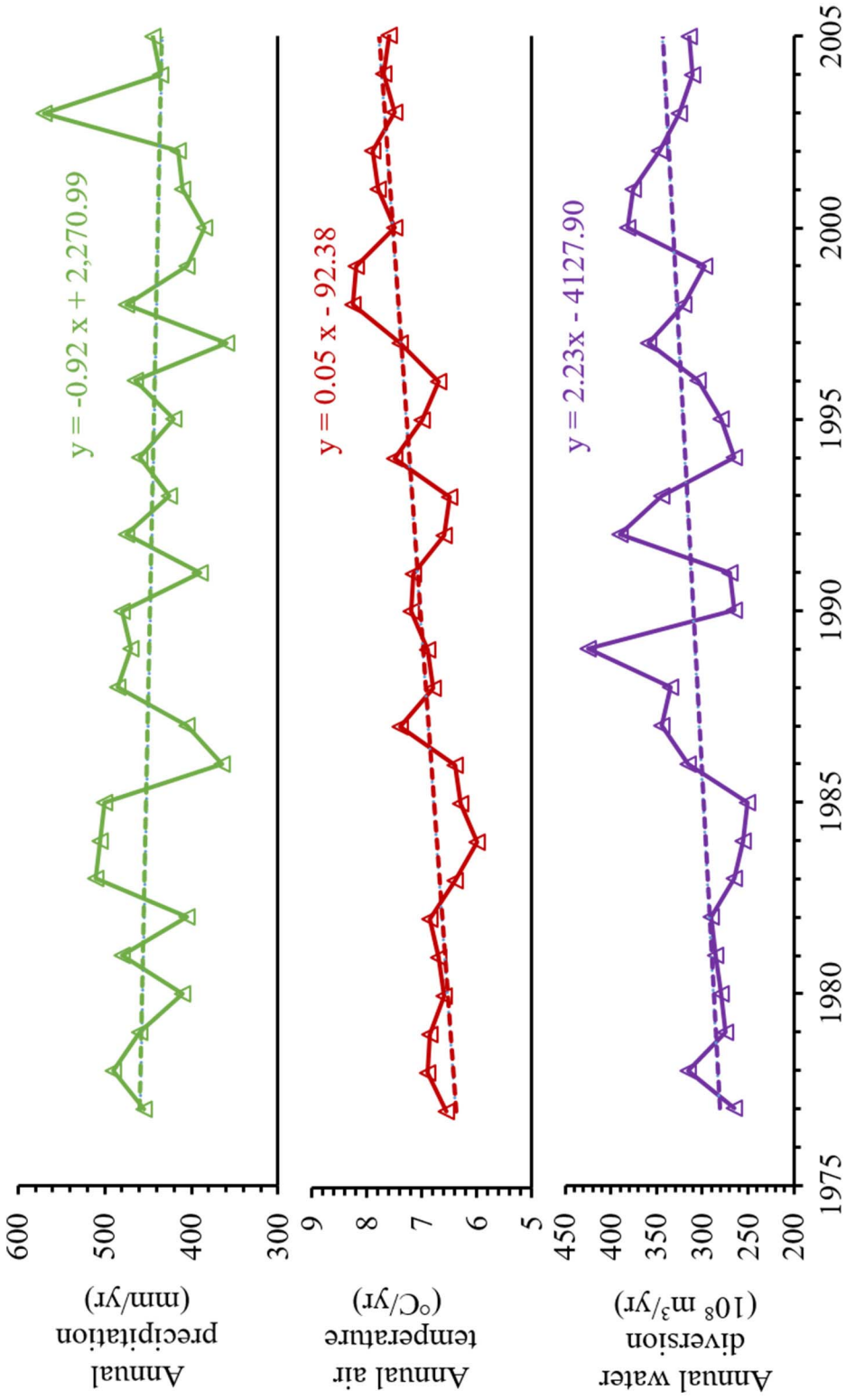

Fig. 6. Temporal variations of basin-scale average annual precipitation, air temperature and water diversion from 1977 to 2005.

Table 3
Correlation coefficient matrix among all the variables.

	P	T	Q_d	Q
P	1	− 0.25	− 0.24	0.63**
T	− 0.25	1	0.31	− 0.67**
Q_d	− 0.24	0.31	1	− 0.58**
Q	0.63**	− 0.67**	− 0.58**	1

** At a significance level of $p < 0.01$.

At the decadal timescale, the landform evolution of the YRD during 1977–2005 has successively gone through a quick accumulation stage (I) in 1977–1985, a stable accumulation stage (II) in 1986–1995 and a slow accumulation stage (III) in 1996–2005. Based on the measured datasets and abovementioned established associations, we can quantitatively illustrate the contributions from both natural and human-induced environmental changes to the decadal transitions of the morphological evolution. Table 4 shows the average annual volumetric changes, precipitations, air temperatures and water diversions over those three decades. From Table 4, the average annual morphological change from stage (I) to stage (II) declined by 1.92×10^8 m^3/yr; meanwhile, the average annual precipitation fell by 30.83 mm/yr, the average annual air temperature increased by 0.38 °C/yr, and the average annual water diversion increased by 47.94×10^8 m^3/yr. From stage (II) to stage (III), the average annual morphological change decreased -2.81×10^8 m^3/yr while the average annual precipitation, air temperature and water diversion varied by − 1 mm/yr, 0.71 °C/yr and 10.2×10^8 m^3/yr, respectively.

Table 4
Average annual volumetric change, precipitation, air temperature and water diversion in different decades.

Periods	Average annual volumetric change (10^8 m^3/yr)	Average annual precipitation (mm/yr)	Average annual air temperature (°C/yr)	Average annual water diversion (10^8 m^3/yr)
1977–1985	5.72	468.33	6.57	275.56
1986–1995	3.80	437.50	6.95	323.50
1996–2005	0.99	436.50	7.66	333.70

According to Eq. (5), we estimated that the changes of the average annual precipitation, air temperature and water diversion contributed 1.23, 0.93 and 0.48×10^8 m^3/yr, respectively, to the decline of the average annual volumetric change from stage (I) to stage (II). The total induced reduction amounted to 2.64×10^8 m^3/yr, which is in good agreement with the observed decrease. Assuming that the total contribution from the changes of each of the three drivers to the change of the deltaic accumulation rate was 100%, the relative contributions of rainfall, air temperature and water diversion to the decline of the volumetric change rate from stage (I) to stage (II) were calculated as 46.59%, 35.23% and 18.18%, respectively, by considering their induced reductions as weights (Fig. 8). Similarly, we evaluated that the decrease of precipitation, the increase of air temperature and the growth of water diversion from stage (II) to stage (III) accounted for reductions of 0.04, 1.77 and 0.10×10^8 m^3/yr of the average annual volumetric change, respectively, and that their total contribution was

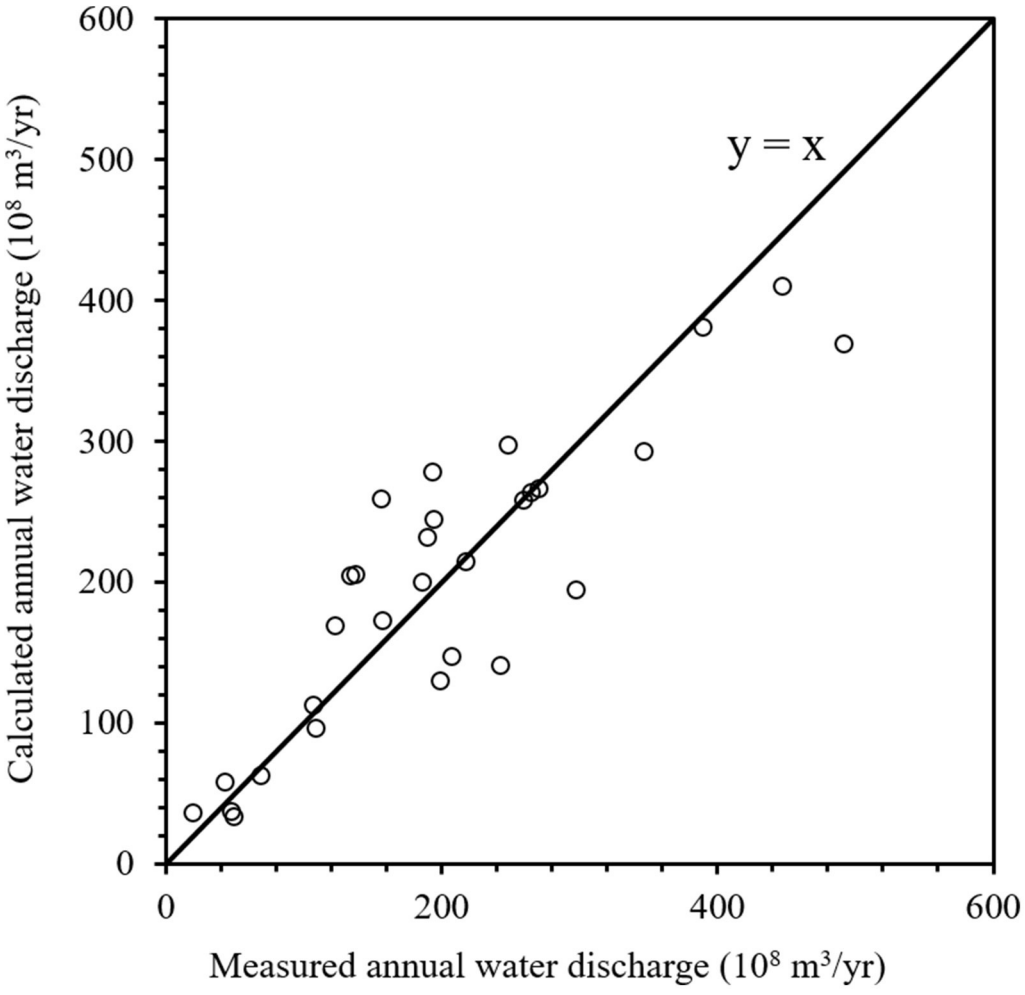

Fig. 7. Comparison between the observed and regressed annual water discharges.

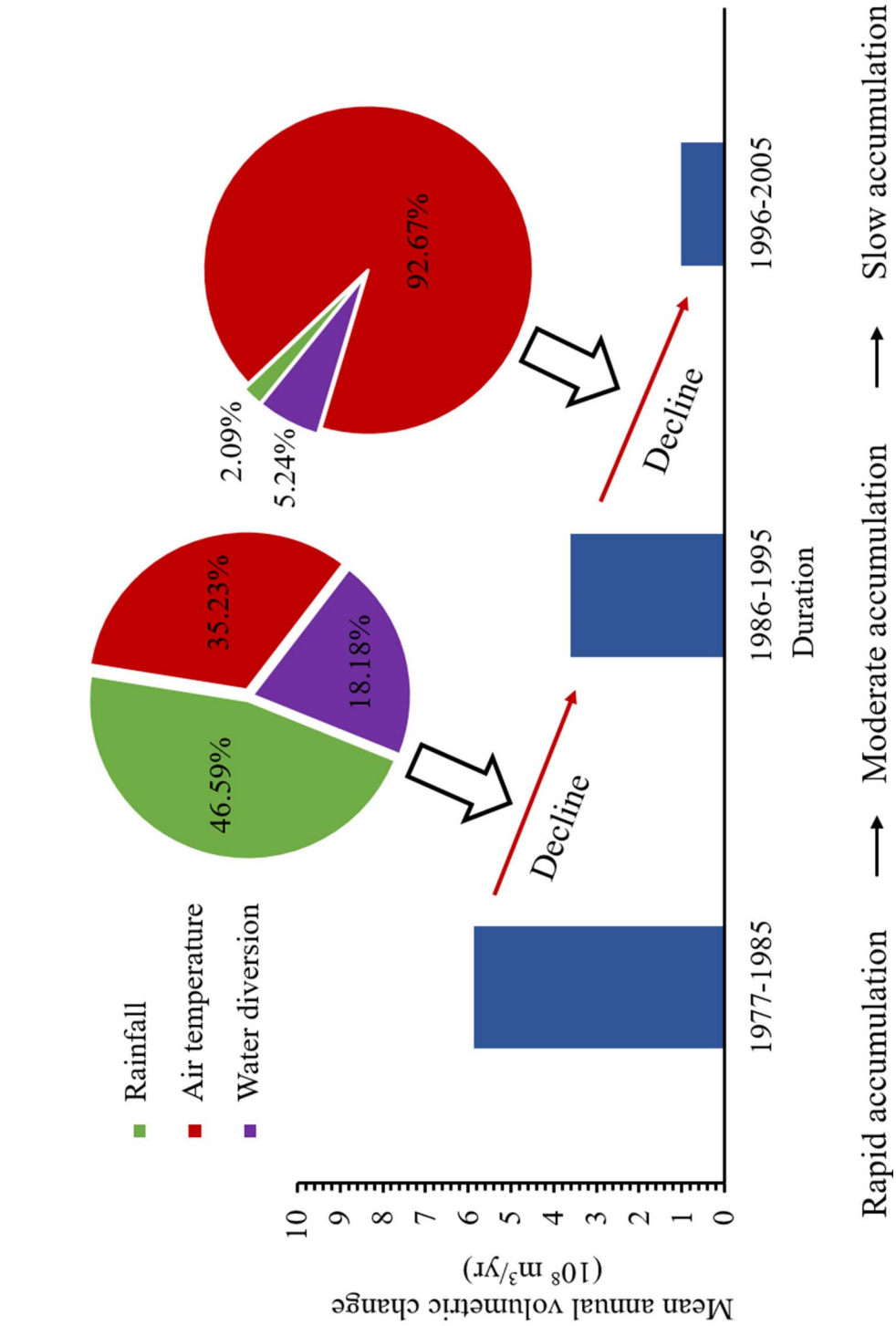

Fig. 8. Contributions of rainfall, air temperature and water diversion to the decreases of decadal morphological change rate.

1.91×10^8 m^3/yr, which represents most of the actual decline. Upon further calculation, it was determined that the rainfall, air temperature and water diversion can explain 2.09%, 92.67% and 5.24%, respectively, of the decline of the volumetric change rate from stage (II) to stage (III) (Fig. 8). The above quantification indicates that the contributions from the rainfall, air temperature and water diversion to the decrease of the average annual morphological change from stage (I) to stage (II) ranked first, second and third, respectively. From stage (II) to stage (III), the rise of air temperature contributed the most to the abovementioned decrease, and the contribution from air temperature was much greater than that from either the decrease of precipitation or the increase of water diversion. Further calculation revealed that the natural and anthropogenic contributions to the transition from stage (I) to stage (II) were 81.82% and 18.18%, respectively, and those to the subsequent transition to stage (III) were 94.76% and 5.24%, respectively. Over the period of 1977–2005, the impact of natural environmental changes within the Yellow River catchment on the inter-decadal variation of the morphological evolution were much higher than that of human-induced change.

5. Discussion

Despite the lack of up-to-date bathymetric survey data, our study examined the morphological response of the fluvial-dominated YRD to both natural and human-induced environmental changes during the period of 1977–2005. As clearly demonstrated above, the variation of the geomorphic evolutionary character of the YRD critically depended upon river hydrological change. Given the diagnosed close water-sediment relationship, the river water flux was considered the representative of hydrological environment. Using the flow discharge as a link, the rainfall and earth surface air temperature in addition to the water diversion projects throughout the Yellow River watershed were identified as the dominant drivers of the transformation of the YRD. Rainfall provides a river system with a major water source and thus controls the runoff generation, channel bed evolution and sediment delivery as well as the deltaic transformation (Gerten et al., 2008; Liu et al., 2016; Rose et al., 2015). Earth surface air temperature significantly affects basin-scale evaporation from water bodies, moist soil and vegetation, evaporation-related water consumption and snow/glacier melt water, thereby altering the river regime and deltaic land accretion (Cuo et al., 2013; Lewis and Allen, 2016; Liu and Cui, 2011; Liu and McVicar, 2012). Compared with the evapotranspiration throughout the Yellow River watershed, the water sourced from snowmelt from the source region was very limited (Cuo et al., 2013). It is clear from Table 2 that there is no significant correlation between the precipitation and air temperature in the Yellow River basin; this is primarily for the following reasons: 1) the summer monsoon delivers vast quantities of vapours from the ocean into the catchment, thereby providing the majority of vapour sources for rainfall, and precipitation is closely related to the intensity of the summer monsoon; 2) inland prevailing winds transport abundant evaporation-induced vapour across the catchment into the adjacent area of river basin (Liu and McVicar, 2012; Wang et al., 2006a, 2006b; Xu, 2008). Water diversion projects for domestic, agricultural and industrial uses in addition to reservoir storage has a direct effect on the water loss of a river system, thereby influencing the fluvial sediment load and deltaic evolution (Syvitski and Milliman, 2007; Walling, 2006). Based on the implementation date (2002) of the water-sediment regulation scheme at the Xiaolangdi Reservoir, we dismissed its effect on water-sediment relation within the Yellow River and the sedimentary process of the YRD during 1977–2005. The potential effects of the spatial distributions of the precipitation, air temperature and water diversion on the sediment yield within the catchment and on the morphological evolution of the estuary in consideration of complex sediment transport processes, such as water-sediment exchange, sedimentation, and re-suspension (Syvitski and Milliman, 2007; Walling and Fang, 2003), were also neglected in this study. Recent studies have shown that coastal environmental changes, which include the manifestations of global sea-level rise, local land subsidence, and the regional wave climate and tidal regime, could also play critical roles in addition to basin controls on the deltaic evolution by altering the underlying surface conditions and sedimentary processes (Higgins et al., 2013; Ren, 1990; Wright, 1977). Ren (1990) documented that the mean rate of sea-level rise ranged from 4.5 to 5.5 mm/yr throughout the YRD and that the mean rate of land subsidence varied from 3 to 4 mm/yr. In contrast to the average annual bathymetric change (0.1 m/yr) during 1977–2005, the relative errors caused by sea-level rise and land subsidence were limited. Extreme storm surges off the river mouth generated by typhoons and cold-wave processes could induce large inter-seasonal variations in estuarine erosion and deposition, which strongly affect longer-term topographic changes (Dai et al., 2014). Under the influences of global climate change, the occurrence frequencies of extreme typhoon and cold-wave events throughout the YRD have increased somewhat over the past several decades (Li and Li, 2011). The tidal shear front off the Yellow River mouth constitutes a crucial factor for deltaic sedimentation, which could be significantly changed by the estuarine morphology (Li et al., 2011; Wang et al., 2017). For a more comprehensive understanding of the association between the basin and deltaic processes, further investigations should take the effects of the operation of the Xiaolangdi Reservoir, the spatial distributions of basin drivers and coastal environmental changes into consideration.

The present study reveals that inter-annual variation of the morphological change of the YRD since the late 1970s has been strongly associated with natural environmental changes within the Yellow River catchment, particularly with respect to precipitation variations. In some river systems without intensive human disturbances, climate oscillations represent a primary cause for changes in the transported load of terrestrial materials into the ocean (Liu et al., 2017; Wang et al., 2011). Lu (2004) and Tian et al. (2016) both indicated that the fluvial sediments transported by large rivers in North China such as the Yellow River appear to be extremely vulnerable to climatic variabilities, which accordingly affect the inter-annual variations of deltaic geomorphological processes. Glantz et al. (1991) concluded that El Nino/Southern Oscillation (ENSO) events resulted in inter-annual fluctuations in the runoff and in the patterns of flooding and drought among different areas worldwide through the teleconnections between coupled ocean-atmosphere circulation systems. Wang et al. (2006a, 2006b) linked ENSO events (1950–2000) to the Eastern Asian summer monsoon and precipitation over the Yellow River drainage basin and reported that the higher frequency and strength of ENSO events could lead to a weaker summer monsoon and lower regional precipitation. According to a wavelet analysis of monthly sea surface temperature data, Liu et al. (2012) found a highly significant inter-annual (2- to 4-year) oscillatory periodicity of ENSO events. Here, we highlight that rainfall fluctuations characterized by the ENSO can make an extremely striking contribution to long-term inter-annual variations of the geomorphic evolution of the river-dominated delta.

The above quantification also indicates that natural environmental changes within the Yellow River catchment during 1977–2005 were the primary cause for the transitions of the decadal landform evolution of the YRD from rapid accumulation (I) to stable accumulation (II) and subsequently to slow accumulation (III). In addition, the impacts of rainfall and water diversion on the inter-decadal changes of the deltaic evolution declined dramatically over time while those of the air temperature increased markedly. The sharp decrease in precipitation from stage (I) to stage (II) was most likely due to a higher frequency occurrence of stronger global ENSO events (Wang et al., 2006b; Wang and Geng, 1999), while the remarkable increase of water diversion was closely related to the operation of the Longyangxia Reservoir in the upper reaches (Chen, 1998; Ran et al., 2010). The slight decrease of precipitation from stage (II) to stage (III) occurred as a result of the relative stability of the magnitude and occurrence frequency of ENSO

events (Wang et al., 2006b; Wang and Geng, 1999), while the slow increase of water diversion was attributable to the inability of newly constructed, large-scale hydraulic projects to considerably diminish the river discharge (Hu et al., 2008). In contract to the changing patterns of the rainfall and water diversion, the air temperature maintained a high warming rate from stage (I) to stage (II) and subsequently to stage (III), which is documented by Kong et al. (2015), Tian et al. (2016) and Yao and Wu (2014) as well. The persistent and rapid increase of earth surface air temperature throughout the Yellow River catchment appears to be closely related to global climate warming (Jones et al., 1999). Evaporation enhanced by incremental temperature changes has played a critically important role in the inter-decadal change of the deltaic transformation since the late 1970s. Based upon an analysis of 60 years of sediment load observations from the route of the Yellow River over China's LP, Wang et al. (2015) concluded that the implementation of landscape engineering and terracing in addition to the construction of check dams and reservoirs were the primary factors that drove the reduction of the sediment load from the 1970s to 1990s and that large-scale vegetation restoration projects reduced the soil erosion beginning in the 1990s. Their study mainly focused on the impacts of human interventions on the decline of the sediment load at the Tongguan and Taodaoguai stations in the LP located in the middle reaches of the Yellow River thousands of kilometres away from the Yellow River estuary. Due to the complex sediment transport processes in the lower reaches, the human impacts on the reduction of the sediment load in the middle reaches may not be able to represent their actual effects on the decreased sediment load into the Bohai Sea. In addition, previous investigations neglected the potential effects of reductions of the water discharge on the sediment load. Wang et al. (2007) indicated that the noticeable reduction of the sediment discharge of the Yellow River from the period of 1950–1968 to the period of 1969–1985 mainly resulted from a decreased water supply induced by human interventions in the river basin, particularly the joint operations of the Sanmenxia and Liujiaxia Reservoirs and water-soil conservation practices. It is thus inferred that the changes of the morphological evolution of the YRD over these two periods were predominantly controlled by basin-scale human-induced environmental changes. Meanwhile, the present study suggests that the inter-decadal change of the deltaic evolution of the YRD during 1977–2005 were dominated by basin-scale natural environmental changes. This comparison demonstrates that the dominant cause of the deltaic evolution shifted from changes of human activity to changes of the natural environment throughout the watershed and that this shift likely occurred in the 1980s. The water-sediment relationship at the LJHS has significantly changed since the implementation of the water-sediment regulation scheme at the Xiaolangdi Reservoir in 2002, and the intensive scouring in the lower reaches has resulted in relatively coarser fluvial sediments, which could be conducive to deltaic progradation (Bi et al., 2014a, 2014b; Fan et al., 2018; Wu et al., 2015). Nevertheless, the accumulation rate of the YRD is likely to continuously decline over the next few decades for the following reasons: 1) the rainfall will maintain a slightly changing trend in the arid and semi-arid zones in the middle and upper reaches of the Yellow River basin (Wang et al., 2006b; Wang and Li, 1990); 2) the earth surface air temperature within the catchment will continue to rise rapidly (Tian et al., 2016; Wang et al., 2006b); and 3) basin-scale water abstraction projects will remain at a high intensity and retain a slow increase (Vörösmarty et al., 2000). Under the long-term effects of regional natural environmental changes, the delta appears to exhibit a tendency of transitioning from progradation to recession at the decadal timescale, thereby triggering the serious destruction of land resources, coastal infrastructures and rich wetland ecosystems as well as of the services the wetland provides (e.g., storm protection, nutrient and pollution removal, and carbon storage).

Numerous previous studies conducted for large deltas worldwide such as the Mississippi River Delta, the Yangtze River Delta, the Mekong River Delta and the Pearl River Delta have noted abrupt and radical human impacts on the deltaic transformation from the construction of large hydraulic structures and the implementation of water diversion projects in the river basin (Anthony et al., 2015; Blue and Roberts, 2009; Wu et al., 2016; Yang et al., 2011); however, such studies more often than not neglected concomitant and persistent natural impacts. Our quantification reveals that inter-annual and inter-decadal changes of the deltaic geomorphic evolution can also be strongly affected by natural environmental changes over a long time frame when human interventions throughout the watershed remain at a relatively stable level. Currently, with the effective utilization and strict management of water resources and a substantial variability of the natural processes in river basins, it is of profound importance to pay close attention to natural impact on further changes of the ecological and geomorphic evolutionary characteristics of deltaic systems.

6. Conclusions

As a typically fluvial-dominated delta, the geomorphological processes of the YRD have been receiving extensive international attention, especially under the influences of considerable environmental changes within the Yellow River catchment. Based on long-term measurements constituting hydro-meteorological and bathymetric data, the basin-scale natural and human impacts on the morphological evolution of the YRD during 1977–2005 are quantitatively examined in this study. The main findings are summarized as follows:

1) Corresponding to variations of the fluvial input, the annual morphological change of the YRD has experienced a distinct decrease coincident with substantial inter-annual variations. The decadal geomorphic evolution has successively gone through three stages, namely, rapid accumulation in 1977–1985, stable accumulation in 1986–1995 and slow accumulation in 1996–2005.
2) The deltaic transformation is strongly associated with the rainfall and earth surface air temperature and in addition to water diversion projects throughout the watershed; the annual volumetric change successively decreases with a decrease of the annual precipitation, an increase of the annual air temperature and an increase of the annual water abstraction.
3) In terms of the magnitude of the effect on the inter-annual variation of the deltaic evolution, the rainfall ranked first (i.e., rainfall had the greatest impact), followed by the air temperature and finally and the water diversion projects.
4) The contributions from rainfall, air temperature and water diversion to the transition of the deltaic decadal evolution from rapid accumulation to stable accumulation ranked first, second and third, respectively. The rapid rise of air temperature contributed the most to the subsequent transition from stable accumulation to slow accumulation, and the contribution from the air temperature was much greater than that from either the decrease of precipitation or the increase of water diversion.

The thorough quantification achieved herein is imperative for a preliminary comprehension of the intensified vulnerability of the YRD induced primarily by natural processes, and the results presented in this study can provide policy makers with valuable quantitative references for solutions to mitigate such vulnerabilities. Furthermore, the YRD can be regarded as a typical case for river deltas that are currently being subjected to enormous effects at the catchment scale, thereby delineating the direction for future research with regard to the fates of deltaic physical environments.

Acknowledgements

This study was financially supported by the National Key Research and Development Program of China (2017YFC0405503), the National Natural Science Foundation of China (U1706214), the Open Research

Fund (ORF) of the State Key Laboratory of Estuarine and Coastal Research (SKLEC-KF201503), and the joint PhD programme of the China Scholarship Council (201306140135) for Overseas Studies. The authors would like to express our gratitude to the Yellow River Water Conservancy Commission of China for the hydrological and bathymetric data, to the China Meteorological Administration for the meteorological data, and to the Earth Resources Observation and Science (EROS) Center for the remote-sensing images. The authors also thank Xiaoxi Liu, Feng Liu and Samuel Bray for their useful comments on the manuscript.

References

Anthony, E.J., Brunier, G., Besset, M., Goichot, M., Dussouillez, P., Nguyen, V.L., 2015. Linking rapid erosion of the Mekong River delta to human activities. Sci. Rep. 5, 14745.
Bi, N.S., Wang, H.J., Yang, Z.S., 2014a. Recent changes in the erosion-accretion patterns of the active Huanghe (Yellow River) delta lobe caused by human activities. Cont. Shelf Res. 90, 70–78.
Bi, N.S., Yang, Z.S., Wang, H.J., Xu, C.L., Guo, Z.G., 2014b. Impact of artificial water and sediment discharge regulation in the Huanghe (Yellow River) on the transport of particulate heavy metals to the sea. Catena 121, 232–240.
Blue, M.D., Roberts, H.H., 2009. Drowning of the Mississippi Delta due to insufficient sediment supply and global sea-level rise. Nat. Geosci. 2, 488–491.
Chen, J., 1998. Regulation of the Yellow River and the Utilization of Water Resources. The Yellow River Water Conservancy Press, Zhengzhou, China.
Chen, J.S., Wang, F.Y., Meybeck, M., He, D.W., Xia, X.H., Zhang, L.T., 2005. Spatial and temporal analysis of water chemistry records (1958–2000) in the Huanghe (Yellow River) basin. Glob. Biogeochem. Cycles 19, GB3016.
Cheng, Y.J., Cheng, J.G., 2000. Analysis of the current field in the new Yellow River entrance sea area. Coast. Eng. 19, 5–11 (in Chinese with English abstract).
Chu, Z.X., Sun, X.G., Zhai, S.K., Xu, K.H., 2006. Changing pattern of accretion/erosion of the modern Yellow River (Huanghe) subaerial delta, China: based on remote sensing images. Mar. Geol. 227, 13–30.
Cui, B.L., Li, X.Y., 2011. Coastline change of the Yellow River estuary and its response to the sediment and runoff (1976–2005). Geomorphology 127, 32–40.
Cui, G.Z., Zhang, X.L., Zhang, Z.H., Xu, Z.J., 2013. Changes of coastal wetland ecosystems in the Yellow River Delta and protection countermeasures to them. Asian Agric. Res. 1, 48–55.
Cuo, L., Zhang, Y.X., Gao, Y.H., Hao, Z.C., Cairang, L., 2013. The impacts of climate change and land cover/use transition on the hydrology in the upper Yellow River Basin, China. J. Hydrol. 502, 37–52.
Dai, Z.J., Liu, J.T., Wei, W., Chen, J.Y., 2014. Detection of the three Gorges Dam influence on the Changjiang (Yangtze River) submerged delta. Sci. Rep. 4, 6600.
Elliott, T., 1989. Deltaic systems and their contribution to an understanding of basin-fill successions. Geol. Soc. Lond. Spec. Publ. 41, 3–10.
Fagherazzi, S., Edmonds, D.A., Nardin, W., Leonardi, N., Canestelli, A., Falcini, F., Jerolmac, D.J., Mariotti, G., Rowland, J.C., Slingerland, R.L., 2015. Dynamics of river mouth deposits. Rev. Geophys. 53, 642–672.
Fan, Y.G., Zhang, S.Q., Hou, C.L., Zhang, L., 2009. Study on method of coastline extraction from remote sensing-taking yellow river mouth reach and Dialkou reach of yellow river delta area as an example. Remote Sens. Inf. 4, 67–70 (in Chinese with English abstract).
Fan, Y.S., Chen, S.L., Zhao, B., Pan, S.Q., Jiang, C., Ji, H.Y., 2018. Shoreline dynamics of the active Yellow River delta since the implementation of water-sediment regulation scheme: a remote-sensing and statistics-based approach. Estuar. Coast. Shelf Sci. 200, 406–419.
Galal, E.M., Takewaka, S., 2011. The influence of alongshore and cross-shore wave energy flux on large- and small-scale coastal erosion patterns. Earth Surf. Process. Landf. 36, 953–966.
Gerten, D., Rost, S., Bloh, W., Lucht, W., 2008. Causes of change in 20th century global river discharge. Geophys. Res. Lett. 35, L20405.
Giosan, L., Syvitski, J., Constantinescu, S., Day, J., 2014. Protect the world's deltas. Nature 516, 31–33.
Glantz, M.H., Katz, R.W., Nicholls, N., 1991. Teleconnections Linking World Wide Climatic Anomalies. Cambridge University Press, Cambridge, UK.
He, C.G., Li, X.J., Zuo, X.L., 2017. Analysis and research on sediment bulk density test in coastal area of Yellow River estuary. Water Res. Dev. Manag. 4, 70–76 (in Chinese with English abstract).
Higgins, S., Overeem, I., Tanaka, A., Syvitski, J.P., 2013. Land subsidence at aquaculture facilities in the Yellow River delta, China. Geophys. Res. Lett. 40, 3898–3902.
Holligan, P.M., Boois, H.D., 1993. Land ocean interactions in the coastal zone (LOICZ). Science plan. In: Global Change Report (Sweden).
Hu, C.H., Ji, Z.W., Wang, T., 1996. Characteristics of ocean dynamics and sediment diffusion in the Yellow River estuary. J. Sediment. Res. 4, 1–10 (in Chinese with English abstract).
Hu, C.H., Chen, X.J., Chen, J.G., 2008. Spatial distribution and its variation process of sedimentation in Yellow River. J. Hydraul. Eng. 39, 518–527 (in Chinese with English abstract).
Jiang, C., Pan, S.Q., Chen, S.L., 2017. Recent morphological changes of the Yellow River (Huanghe) submerged delta: causes and environmental implications. Geomorphology 293, 93–107.
Jones, P.D., New, M., Parker, D.E., Martin, S., Rigor, I.G., 1999. Surface air temperature and its changes over the past 150 years. Rev. Geophys. 37, 173–199.
Kong, D.X., Miao, C.Y., Borthwick, A.G.L., Duan, Q.Y., Liu, H., Sun, Q.H., Ye, A.Z., Di, Z.H., Gong, W., 2015. Evolution of the Yellow River Delta and its relationship with runoff and sediment load from 1983 to 2011. J. Hydrol. 520, 157–167.
Lespinas, F., Ludwig, W., Heussner, S., 2014. Hydrological and climatic uncertainties associated with modeling the impact of climate change on water resources of small Mediterranean coastal rivers. J. Hydrol. 511, 403–422.
Lewis, C.S., Allen, L.N., 2016. Potential crop evapotranspiration and surface evaporation estimates via a gridded weather forcing dataset. J. Hydrol. 546, 450–463.
Li, W.Y., Gong, P., 2016. Continuous monitoring of coastline dynamics in western Florida with a 30-year time series of Landsat imagery. Remote Sens. Environ. 179, 196–209.
Li, K., Li, G.S., 2011. Progress in research on risk of storm surge. J. Nat. Dis. 20 (6), 104–111 (in Chinese with English abstract).
Li, G.X., Tang, Z.S., Yue, S.H., Zhang, K.L., Wei, H.L., 2011. Sedimentation in the shear front off the Yellow River mouth. Cont. Shelf Res. 21, 607–625.
Liu, Q., Cui, B.S., 2011. Impacts of climate change/variability on the streamflow in the Yellow River Basin, China. Ecol. Model. 222 (2), 268–274.
Liu, Q., McVicar, T.M., 2012. Assessing climate change induced modification of penman potential evaporation and runoff sensitivity in a large water-limited basin. J. Hydrol. 464-465, 352–362.
Liu, F., Chen, S.L., Dong, P., Peng, J., 2012. Spatial and temporal variability of water discharge in the Yellow River Basin over the past 60 years. J. Geogr. Sci. 22, 1013–1033.
Liu, F., Yang, Q.S., Chen, S.L., Luo, Z.F., Yuan, F., Wang, R.T., 2014a. Temporal and spatial variability of sediment flux into the sea from the three largest rivers in China. J. Asian Earth Sci. 87, 102–115.
Liu, F., Yuan, L.R., Yang, Q.S., Ou, S.Y., Xie, L.L., Cui, X., 2014b. Hydrological responses to the combined influence of diverse human activities in the Pearl River delta, China. Catena 113, 41–55.
Liu, Y.J., Yang, J., Hu, J.M., Tang, C.J., Zhang, H.J., 2016. Characteristics of the surface-subsurface flow generation and sediment yield to the rainfall regime and land-cover by long-term in-situ observation in the red soil region, Southern China. J. Hydrol. 539, 457–467.
Liu, F., Chen, H., Cai, H.Y., Luo, X.X., Ou, S.Y., Yang, Q.S., 2017. Impacts of ENSO on multi-scale variations in sediment discharge from the Pearl River to the South China Sea. Geomorphology 293, 24–36.
Lu, X.X., 2004. Vulnerability of water discharge of large Chinese rivers to environmental changes: an overview. Reg. Environ. Chang. 4, 182–191.
Meade, R.H., Moody, J.A., 2010. Causes for the decline of suspended-sediment discharge in the Mississippi River system, 1940–2007. Hydrol. Process. 24, 35–49.
Milliman, J.D., Meade, R.H., 1983. World-wide delivery of river sediment to the oceans. J. Geol. 91 (1), 1–21.
Overeem, I., Brakenridge, R.G., 2009. Dynamics and Vulnerability of Delta Systems. GKSS Research Centre, LOICZ International Project Office, Institute for Coastal Research.
Pang, J.Z., Si, S.H., 1979. Evolution of the Yellow River mouth: I. Historical shifts. Oceanol. Limnol. Sin. 10 (2), 136–141 (in Chinese with English abstract).
Pang, A.P., Sun, T., Yang, Z.F., 2013. Economic compensation standard for irrigation processes to safeguard environmental flows in the Yellow River Estuary, China. J. Hydrol. 482, 129–138.
Peng, J., Chen, S.L., 2010. Response of delta sedimentary system to variation of water and sediment in the Yellow River over past six decades. J. Geogr. Sci. 20, 613–627.
Peng, J., Chen, S.L., Dong, P., 2010. Temporal variation of sediment load in the Yellow River basin, China, and its impacts on the lower reaches and the river delta. Catena 83, 135–147.
Peng, J., Ma, S., Chen, H., Li, Z., 2013. Temporal and spatial evolution of coastline and subaqueous geomorphology in muddy coast of the Yellow River Delta. J. Geogr. Sci. 23, 490–502.
Qiao, S.Q., Shi, X.F., Saito, Y., Li, X.Y., Yu, Y.G., Bai, Y.Z., Liu, Y.G., Wang, K.S., Yang, G., 2011. Sedimentary records of natural and artificial Huanghe (Yellow River) channel shifts during the Holocene in the southern Bohai Sea. Cont. Shelf Res. 31, 1336–1342.
Ran, L.S., Wang, S.J., Fan, X.L., 2010. Channel change at Toudaoguai Station and its responses to the operation of upstream reservoirs in the upper Yellow River. J. Geogr. Sci. 20, 231–247.
Ren, M.E., 1990. Effect of sea level rise and land subsidence on the Huanghe River delta. Sci. Geogr. Sin. 10 (1), 48–57.
Ren, M.E., Shi, Y.L., 1986. Sediment discharge of the Yellow River (China) and its effect on the sedimentation of the Bohai and the Yellow Sea. Cont. Shelf Res. 6, 785–810.
Rose, C.W., Shellberg, J.G., Brooks, A.P., 2015. Modelling suspended sediment concentration and load in a transport-limited alluvial gully in northern Queensland, Australia. Earth Surf. Process. Landf. 40, 1291–1303.
Ryu, J.H., Won, J.S., Min, K.D., 2002. Waterline extraction from Landsat TM data in a tidal flat: a case study in Gomso Bay, Korea. Remote Sens. Environ. 83, 442–456.
Saito, Y., Yang, Z.S., Hori, K., 2001. The Huanghe (Yellow River) and Changjiang (Yangtze River) deltas: a review on their characteristics, evolution and sediment discharge during the Holocene. Geomorphology 41, 219–231.
Santos, R.M.B., Sanches Fernandes, L.F., Moura, J.P., Pereira, M.G., Pacheco, F.A.L., 2014. The impact of climate change, human interference, scale and modeling uncertainties on the estimation of aquifer properties and river flow components. J. Hydrol. 519 (B), 1297–1314.
Serra, P., Pons, X., Sauri, D., 2003. Post-classification change detection with data from different sensors: some accuracy considerations. Int. J. Remote Sens. 24, 3311–3340.
Sun, X.G., Yang, Z.S., Chen, Z.R., 1993. The calculation and regularity discussion of silt erosion/deposition in modern Yellow River mouth area. Acta Oceanol. Sin. 15, 129–136 (in Chinese with English abstract).
Sun, Q.H., Miao, C.Y., Duan, Q.Y., Kong, D.X., Ye, A.Z., Di, Z.H., Gong, W., 2014. Would

the 'real' observed dataset stand up? A critical examination of eight observed gridded climate datasets for China. Environ. Res. Lett. 9, 015001.
Sun, Z.G., Mou, X.J., Tong, C., Wang, C.Y., Xie, Z.L., Song, H.L., Sun, W.G., Lv, Y.C., 2015. Spatial variations and bioaccumulation of heavy metals in intertidal zone of the Yellow River estuary, China. Catena 126, 43–52.
Syvitski, J.P., 2008. Deltas at risk. Sustain. Sci. 3, 23–32.
Syvitski, J.P., Milliman, J.D., 2007. Geology, geography, and humans battle for dominance over the delivery of fluvial sediment to the coastal ocean. J. Geol. 115, 1–19.
Syvitski, J.P., Kettner, A.J., Overeem, I., Hutton, E.W.H., Hannon, M.T., Brakenridge, G.R., Day, J., Vörösmarty, C., Saito, Y., Giosan, L., Nicholls, R.J., 2009. Sinking deltas due to human activities. Nat. Geosci. 2, 681–686.
Tang, K., 2004. Soil Conservation in China. Press of Science in China, Beijing, China.
Tessler, Z.D., Vörösmarty, C.J., Grossberg, M., Gladkova, I., Aizenman, H., Syvitski, J.P., Foufoula-Georgiou, E., 2015. Profiling risk and sustainability in coastal deltas of the world. Science 349, 638–643.
Tian, Q., Prange, M., Merkel, U., 2016. Precipitation and temperature changes in the major Chinese river basins during 1957–2013 and links to sea surface temperature. J. Hydrol. 536, 208–221.
Vörösmarty, C.J., Green, P., Salisbury, J., Lammers, R.B., 2000. Global water resources: vulnerability from climate change and population growth. Science 289, 284–288.
Walling, D.E., 2006. Human impact on land-ocean sediment transfer by the world's rivers. Geomorphology 79, 192–216.
Walling, D.E., Fang, D., 2003. Recent trends in the suspended sediment loads of the world's rivers. Glob. Planet. Chang. 39, 111–126.
Wang, S., Geng, D., 1999. The ENSO events and their magnitudes over the past 100 years. Meteor-Forschung 25 (1), 9–13 (in Chinese with English abstract).
Wang, W.C., Li, K.R., 1990. Precipitation fluctuation over semiarid region in northern China and the relationship with El Nino/Southern Oscillation. J. Clim. 3, 769–783.
Wang, S.J., Hassan, M.A., Xie, X.P., 2006a. Relationship between suspended sediment load, channel geometry and land area increment in the Yellow River Delta. Catena 65, 302–314.
Wang, H.J., Yang, Z.S., Saito, Y., Liu, J.P., Sun, X.X., 2006b. Interannual and seasonal variation of the Huanghe (Yellow River) water discharge over the past 50 years: connections to impacts from ENSO events and dams. Glob. Planet. Chang. 50, 212–225.
Wang, H.J., Yang, Z.S., Saito, Y., Liu, J.P., Sun, X.X., Wang, Y., 2007. Stepwise decreases of the Huanghe (Yellow River) sediment load (1950–2005): impacts of climate change and human activities. Glob. Planet. Chang. 57, 331–354.
Wang, H.J., Saito, Y., Zhang, Y., Bi, N.S., Sun, X., Yang, Z., 2011. Recent changes of sediment flux to the western Pacific Ocean from major rivers in East and Southeast Asia. Earth Sci. Rev. 108, 80–100.
Wang, W., Shao, Q., Yang, T., Peng, S., Yu, Z., Taylor, J., Xing, W., Zhao, C., Sun, F., 2013. Changes in daily temperature and precipitation extremes in the Yellow River Basin, China. Stoch. Env. Res. Risk A. 27, 401–421.
Wang, S., Fu, B.J., Piao, S.L., Lu, Y.H., Ciais, P., Feng, X.M., Wang, Y.F., 2015. Reduced sediment transport in the Yellow River due to anthropogenic changes. Nat. Geosci. 9, 38–42.
Wang, N., Li, G.X., Qiao, L.L., Shi, J.H., Dong, P., Xu, J.S., Ma, Y.Y., 2017. Long-term evolution in the location, propagation, and magnitude of the tidal shear front off the Yellow River Mouth. Cont. Shelf Res. 137, 1–12.
Wright, L.D., 1977. Sediment transport and deposition at river mouths: a synthesis. Geol. Soc. Am. Bull. 88, 857–868.
Wu, X., Bi, N.S., Yuan, P., Li, S., Wang, H.J., 2015. Sediment dispersal and accumulation off the present Huanghe (Yellow River) delta as impacted by the water-sediment regulation scheme. Cont. Shelf Res. 111 (B), 126–138.
Wu, C.S., Yang, S.L., Huang, S.C., Mu, J.B., 2016. Delta changes in the Pearl River estuary and its response to human activities (1954–2008). Quat. Int. 392, 147–154.
Wu, X., Bi, N.S., Xu, J.P., Nittrouer, J.A., Yang, Z.S., Saito, Y., Wang, H.J., 2017. Stepwise morphologcial evolution of the active Yellow River (Huanghe) delta lobe (1976–2013): dominant roles of riverine discharge and sediment grain size. Geomorphology 292, 115–127.
Xu, J.X., 2002. A study of thresholds of runoff and sediment for the land accretion of the Yellow River Delta. Geogr. Res. 21 (2), 163–170 (in Chinese with English abstract).
Xu, J.X., 2003. Sediment flux into the sea as influenced by the changing human activities and precipitation: example of the Huanghe River, China. Environ. Manag. 31, 328–341.
Xu, J.X., 2005. The water fluxes of the Yellow River to the sea in the past 50 years, in response to climate change and human activities. Environ. Manag. 35, 620–631.
Xu, J.X., 2006. Land accretion of the Yellow River Delta as influenced by drainage basin factors. Geogr. Ann. Ser. A Phys. Geogr. 88, 31–41.
Xu, J.X., 2008. Response of land accretion of the Yellow River delta to global climate change and human activity. Quat. Int. 186, 4–11.
Xu, X.G., Guo, H.H., Chen, X.L., Lin, H.P., Du, Q.L., 2002. A multi-scale study on land use and land cover quality change: the case of the Yellow River Delta in China. GeoJournal 56, 177–183.
Yang, S.L., Milliman, J.D., Li, P., Xu, K., 2011. 50,000 dams later: erosion of the Yangtze River and its delta. Glob. Planet. Chang. 75, 14–20.
Yao, W.Y., Wu, D., 2014. Charateristics and variation trends of temperature and precipitation in the Yellow River basin during 1961–2010. Chin. Rural Water Hydropower 8, 104–114 (in Chinese with English abstract).
Yu, J., Fu, Y., Li, Y., Han, G., Wang, Y., Zhou, D., Sun, W., Gao, Y., Meixner, F., 2011. Effects of water discharge and sediment load on evolution of modern Yellow River Delta, China, over the period from 1976 to 2009. Biogeosciences 8, 2427–2435.
Zhang, G.S., Wang, L.C., Liu, D.S., 1998. Biodiversity and its conservation in the Yellow River Delta nature reserve. Rural Eco-Environ. 14, 16–18 (in Chinese with English abstract).
Zhou, Y.Y., Huang, H.Q., Nanson, G.C., Huang, C., Liu, G.H., 2015. Progradation of the Yellow (Huanghe) River delta in response to the implementation of a basin-scale water regulation program. Geomorphology 243, 65–74.